journal

J. Am. Ceram. Soc., 87 [2] 293–95 (2004)

Directed Colloidal Assembly of Linear and Annular Lead Zirconate Titanate Arrays

James E. Smay,[†,‡,§] Joseph Cesarano III,[‡] Bruce A. Tuttle,[‡] and Jennifer A. Lewis[*,†]

Department of Materials Science and Engineering, University of Illinois, Urbana, Illinois 61802

Sandia National Laboratories, Albuquerque, New Mexico 87185

Lead zirconate titanate (PZT) arrays for ultrasonic sensing applications in the 2–30-MHz frequency range were fabricated by robocasting, a directed colloidal assembly technique. Both linear and annular arrays were produced by robotically depositing a concentrated PZT gel-based ink to create high-aspect-ratio PZT elements (thickness ~ 130 μm and height ~1–2 mm) of varying pitch (~250–410 μm). The arrays were densified and infiltrated with an epoxy resin to fabricate PZT–polymer composites with 2–2 connectivity. Their dielectric and piezoelectric constants were measured and compared with values obtained for bulk PZT and those predicted theoretically.

I. Introduction

PIEZOELECTRIC-BASED ceramics and composites are widely used in hydrostatic sensing applications[1–4] (e.g., sonar) and in diagnostic ultrasound instruments.[5,6] Lead zirconate titanate (PZT) often serves as the active ceramic phase due to its high d_{33} piezoelectric coefficient. PZT–polymer composites offer a lower acoustic impedance than monolithic PZT and the ability to engineering the composite structure to enhance the piezoelectric response. A variety of connectivity designs[7] of PZT–polymer composites have been created, such as: 1–3 (aligned PZT rods embedded in a polymer matrix), 2–2 (interleaved plates or concentric rings of PZT and polymer), and 3–3 (interpenetrating three-dimensional lattice of PZT within the polymer matrix). For ultrasound applications, 2–2 composites,[8,9] consisting of linear and annular arrays of piezoelectric elements, permit ultrasound beam focusing and steering.[5,6] Most ultrasound devices operate in the 2–30-MHz range and require a 50-Ω impedance. For control of acoustic and electrical impedances, critical design parameters include the volume fraction and aspect ratio of the PZT elements, respectively. High-aspect-ratio, thin PZT elements are desirable to increase both the electrical impedance and the operating frequency.

Currently, PZT–polymer composites are commercially fabricated by injection molding, manual alignment of ceramic rods, or dicing of solid ceramic monoliths into discrete elements[4,7] to form the PZT phase followed by embedding in a polymer matrix. Recently, PZT–polymer composites have been demonstrated by solid freeform fabrication techniques, such as fused deposition or robocasting.[10–13] In this paper, the fabrication and characterization of linear and annular PZT arrays produced by robocasting[14,15] are reported. A concentrated colloidal gel-based ink is robotically deposited via a cylindrical nozzle to create three-dimensional structures in a layer-by-layer build sequence. By controlling the viscoelastic properties of the colloidal ink,[16] printed layers can maintain their shape throughout the deposition, drying, and sintering processes. Once formed, these PZT skeletal structures are infiltrated with a polymer phase to produce the desired composite. The PZT skeletal structures possess both feature sizes and electrical properties suitable for sensing applications.

II. Experimental Procedure

Lead zirconate titanate (PZT-5H, Morgan Matroc, Electro Ceramics Division, Bedford, OH) was used in this study. The as-received PZT powder contained ~0.3 wt% poly(methacrylic acid) ammonium salt preadsorbed as a dispersant. Concentrated, colloidal gel-based inks were formulated in a two-step process. First, PZT powder was added to an aqueous NH_4OH solution (pH ~ 10.35) in a high-density polyethylene bottle containing five zirconia milling media (08-412-15C, Fisher Scientific Inc., Pittsburgh, PA), creating a suspension with a solids volume fraction of $\phi_{PZT} = 0.55$. Vigorous shaking of the bottle on a paint shaker (5400, Red Devil Equipment Co., Brooklyn Park, MN) was followed by sonication (XL2020 Sonicator, Misonix, Inc., Farmingdale, NY) for 5 min with a 1-s on/off pulse sequence and a power of ~150 W. Lowering the pH via HNO_3 titration induced gelation of the PZT suspension. Finally, the colloidal gel was vigorously mixed for 1 h. The rheological properties of PZT colloidal gels have been reported in Ref. 16.

The colloidal gel was used as ink in a robotically controlled deposition process using a robocasting apparatus.[14] This device consists of three orthogonal axes of coordinated motion control (DMC-1800, Galil Motion Control, Rocklin, CA) and control software. A syringe filled with the concentrated PZT gel was attached to a blunted hypodermic needle (27 gauge, EFD, Inc., East Providence, RI) and mounted on the vertical axis of the robocasting apparatus for controlled dispensing of the colloidal ink at a volumetric flow rate of ~10 μL/min (i.e., proportional to the nozzle diameter of 150 μm and the deposition speed of 10 mm/s).

Linear (LA) and annular (AA) arrays of high-aspect-ratio PZT elements were created by robotic deposition. LA's were fabricated by sequentially depositing a serpentine fill pattern within a rectangular area (e.g., from the lower-left to the upper-right corner), adjusting the deposition nozzle height ($\Delta z = 130$ μm) and then reversing the fill the pattern to deposit another layer atop the first. AA's were deposited as concentric rings from the outer to the inner diameter in the first layer followed by an inner to outer diameter fill pattern in the second layer. For either structure, a total of 12 layers were deposited. LA and AA dimensions are listed in

B. Derby—contributing editor

Manuscript No. 10417. Received July 29, 2003; approved September 3, 2003.

J.A.L. acknowledges partial support from the U.S. Department of Energy, Division of Materials Sciences through the Frederick Seitz MRL at the University of Illinois. This work was funded by the National Science Foundation (Grant No. DMI 99-01030) and by Sandia, a multiprogram laboratory operated by Sandia Corp., a Lockheed Martin Co., for the United States Department of Energy under Contract DE-AC04-94AL85000.

[*]Member, American Ceramic Society.

[†]University of Illinois.

[‡]Sandia National Laboratories.

[§]Current address: School of Chemical Engineering, Oklahoma State University, Stillwater, Oklahoma 74078.

Table I. Design Parameters for PZT Arrays

Component	Height (mm)	Length or outside radius (mm)	Width or inside radius (mm)	Element spacing (mm)
LA-1	1.80	10	10	0.5
LA-2	1.80	10	10	0.3
AA-1	1.08	10	0.75	0.5
AA-2	2.08	10	1.0	0.3

Table I. As a benchmark, solid PZT disks were formed by cold isostatic pressing at 200 MPa and by robotic deposition.

A water-saturated plaster plate was used as the substrate during deposition. Both the substrate and the PZT arrays were in direct contact with ambient air (~22°C and 30% relative humidity) during deposition. Continuously dispensing a small amount of water onto the substrate surface during deposition kept the plaster plate saturated. After deposition, the substrate and PZT array were allowed to dry for ~4 h. The PZT array was then removed from the substrate and bisque-fired at 700°C for 1 h in an alumina crucible. The arrays were sintered at 1275°C for 2 h on a PZT setter plate enclosed in an alumina crucible with a PZT powder bed for atmosphere control. Sintered density was evaluated by the Archimedes method.[17] The surface roughness of sintered PZT elements was evaluated by noncontact laser profilometry (Model 301K, Keyence Co., Osaka, Japan) and by image analysis of scanning electron micrographs (Hitachi, Pleasanton, CA). PZT–polymer composites were produced by embedding the PZT arrays in an epoxy (Spurrs epoxy, Polysciences, Inc., Warrington, PA) matrix.

After polishing and electroding by gold sputtering, the composites and solid PZT disks were poled at 25 kV/cm for 30 min at room temperature followed by short-circuiting for 1 h to accelerate aging. The dielectric constant (K_3) and tan δ of the samples were measured with an impedance analyzer (HP 4284A precision LCR meter, Yakogama-Hewlett-Packard, Tokyo, Japan) at a frequency of 1 kHz and field strength of 1 V/mm. Additionally, d_{33} measurements were performed using a Berlincourt meter (CPDT3300, Channel Industries, Santa Barbra, CA) with hemispherical contacts.

III. Results and Discussion

Optical images of as-deposited PZT linear and annular arrays are shown in Fig. 1(a). Solid base layers (most evident in LA-2) to aid in handling the PZT arrays before densification are visible in these images. The base layers were removed by grinding after epoxy infiltration. Additionally, various connecting features that were incorporated into the array designs due to the continuous nature of the deposition process are visible. For example, PZT elements are connected in series by the hairpin turns of the serpentine fill pattern in LA's, whereas the concentric PZT cylinders are connected within the AA's by a radial line. The presence of such connections may degrade device performance in ultrasound applications by mechanical coupling between ideally isolated, individually addressed PZT elements. While these features could be removed after epoxy infiltration by grinding (at least for the LA's), an ability to shutter the ink flow during deposition is needed to eliminate the radial line in the AA's. The effect of the connecting features was not assessed in this study.

As-deposited PZT arrays displayed no visible shrinkage, warping, or cracking on drying; a hallmark of highly concentrated gel-based inks that possess a shear yield stress, an equilibrium elastic modulus, and a compressive yield stress (see Ref. 16 for details). These properties allow the deposited structures to maintain their shape during the deposition process without slumping or deformation and to subsequently withstand capillary-induced drying stresses. Optical images of sintered PZT arrays are shown in Fig. 1(b). The linear and radial PZT arrays experienced ~17% linear shrinkage during sintering and possessed a final density of ~98% of theoretical density. The cross-sectional view in Fig. 2 reveals that high-aspect-ratio PZT elements, deposited from a 150-μm diameter nozzle with a 300-μm pitch, were reduced in size to ~130 μm with a ~250-μm pitch on sintering. The sidewall roughness of the PZT elements originates from the sequential deposition of cylindrical ink filaments. The root-mean-squared roughness (see Fig. 2) of the sidewalls was found to be ~8 μm. This value is roughly 5% of the wall width. Its affect on ultrasound device performance was not quantified in this work.

Table II summarizes the volume fraction PZT (ϕ_{PZT}), relative permittivity (ε_r), remanent polarization (P_{rem}), and axial piezoelectric constant (d_{33}) for the four composite structures after epoxy infiltration, electroding, and poling and the monolithic PZT disks formed by cold isostatic pressing (CIP) and robocasting (RC). In all cases, the ε_r and P_{rem} values were directly proportional to the ϕ_{PZT}, as expected. The monolithic disks exhibited comparable ε_r, P_{rem}, and d_{33} values, indicating that the aqueous processing route did not degrade the PZT phase.

For the 2–2 composites, d_{33} values were consistently higher than predicted on the basis of simple ϕ_{PZT} scaling; however, a parallel mixing rule[18] for laminar composites was used to predict the values listed in Table II. This model considers the well-known stress concentration effect resulting from parallel alignment of a stiff phase (PZT) with a compliant phase (polymer). The measured

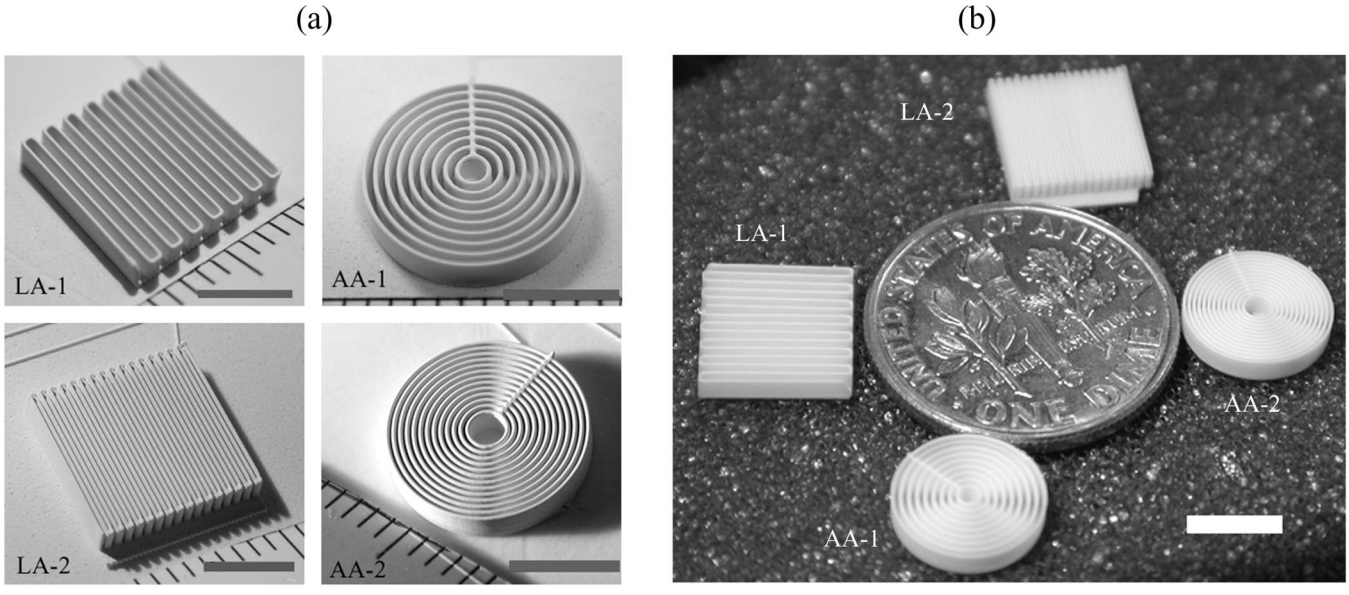

Fig. 1. Optical micrographs of (a) as-dried and (b) sintered linear and annular PZT arrays. All scale bars equal 5 mm.

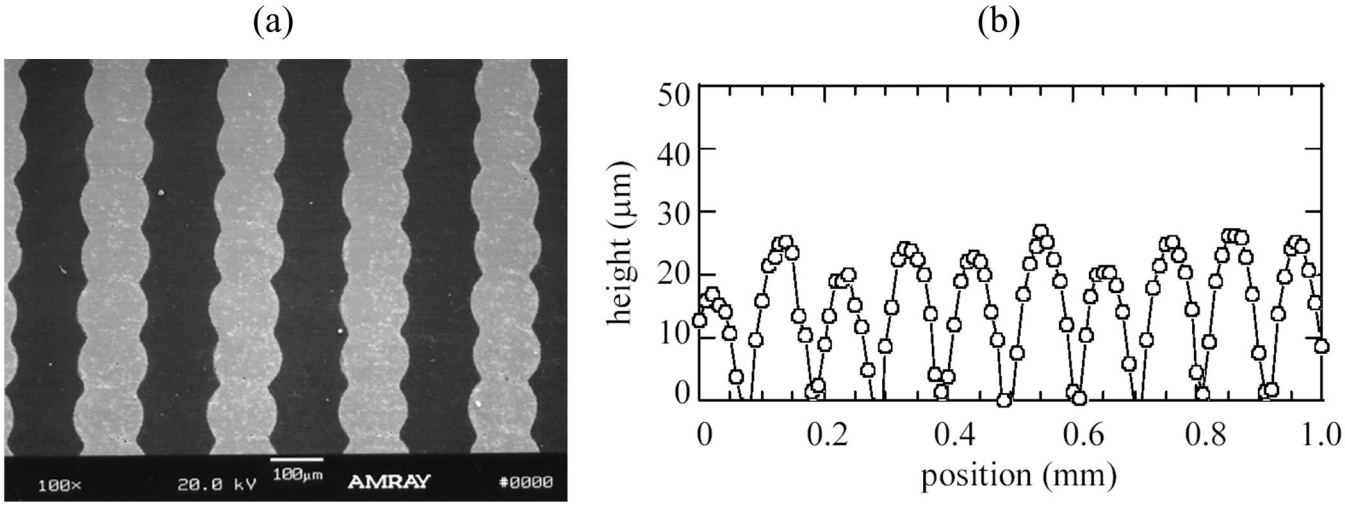

Fig. 2. (a) SEM micrograph of LA-2 array cross section after sintering and epoxy infiltration and (b) profilometry scan taken along one of the side (vertical) walls of the LA-2 array before epoxy infiltration.

Table II. Electrical Properties of PZT Disks and 2–2 PZT–Polymer Composites

Component	ϕ_{PZT}	ε_r †		P_{rem} ($\mu C/m^2$)	d_{33} (pC/N)‡	
		Measured	Calculated		Measured	Calculated
CIP	1	2991		31.5	627	
RC	1	2713		31.8	672	
LA-1	0.31	831	841	7.1	388	633
LA-2	0.55	1492	1492	15.5	330	655
AA-1	0.39	1081	1058	10.0	496	643
AA-2	0.68	1839	1844	17.9	466	660

†Measured at 1 KHz. ‡Measured at 100 Hz.

d_{33} was less than predicted by this theory, which is an indication that, although some stress concentration occurred, it was less than for an ideal parallel composite. The Berlincourt meter uses point contacts for d_{33} measurement, and the reported value is an average of 15 samples collected randomly over the surface of the composite. Some d_{33} values approached that for the RD sample, whereas some showed negligible d_{33}. Presumably, these disparate data correspond to sampling with the point contacts directly over the PZT or polymer phases, respectively. Thus, the PZT phase appeared to be well-poled within the composite and would serve as ultrasound array elements.

The primary focus of this work concerned the fabrication of the PZT arrays and preliminary electrical characterization rather than investigation of their high-frequency properties. For designing an ultrasound array, electrical impedance equalization of the annular array elements is important. Since the electrical impedance of a PZT element is proportional to its height divided by its electroded area, electrical impedance equalization can be readily accomplished by either increasing the element width as the element radius decreases or decreasing the height of the elements with decreasing element radius. The first strategy would provide an equal resonance frequency for each element, whereas the second would result in a higher resonance frequency as the radius decreased. Thus, avenues exist for controlling PZT device architecture for designing ultrasonic array sensors.

IV. Conclusions

Robocasting, a directed colloidal assembly technique, has been demonstrated as a facile approach for creating simple linear and annular PZT arrays on planar substrates. The characterization of these devices indicated that the colloidal-gel-processing route produced a dense ceramic phase with electrical properties comparable to an isopressed derived standard. The primary advantage of this technique is the ability to rapidly vary the array pitch and the number of elements in a sensor. Using this approach, a broad device design space can be quickly assessed to identify optimal structures (e.g., composition, element geometry, and pitch) for use in diagnostic ultrasound devices.

Acknowledgments

We thank Walter Olson of Sandia National Laboratories, Albuquerque, NM, for his assistance with the electrical characterization.

References

[1]K. Rittenmyer, T. Shrout, W. A. Schulze, and R. E. Newnham, "Piezoelectric 3–3 Composites," *Ferroelectrics*, **41** [1–4], 189–95 (1982).
[2]R. E. Newnham, L. J. Bowen, K. A. Klicker, and L. E. Cross, "Composite Piezoelectric Transducers," *Mater. Eng.*, **2**, 93–106 (1980).
[3]R. E. Newnham, "Composites Electroceramics," *Ferroelectrics*, **68**, 1–32 (1986).
[4]J. F. Tressler, S. Alkpu, A. Dogan, and R. E. Newnham, "Functional Composites for Sensors, Actuators and Transducers," *Composites, Part A*, **30A** [4] 477–82 (1999).
[5]W. A. Smith and A. A. Shaulov, "Composite Piezoelectrics: Basic Research to a Practical Device," *Ferroelectrics*, **87**, 309–20 (1988).
[6]T. R. Gururaja, "Piezoelectrics for Medical Ultrasonic Imaging," *Am. Ceram. Soc. Bull.*, **73** [5] 50–55 (1994).
[7]V. F. Janas and A. Safari, "Overview of Fine-Scale Piezoelectric Ceramic/Polymer Composite Processing," *J. Am. Ceram. Soc.*, **78** [11] 2945–55 (1995).
[8]K. Snook, T. R. Shrout, and K. K. Shund, Design of a 50 MHz Annular Array Using Fine-Grain Lead Titanate; pp. 351–54 in *International Symposium on Application of Ferroelectrics* (Nara, Japan). Edited by G. White and T. Tsunumi. Institute of Electrical and Electronics Engineers, New York, 2002.
[9]J. M. Cannata, T. R. Shrout, and K. K. Shung, A 35 MHz Linear Ultrasonic Array for Medical Imaging; pp. 343–46 in *International Symposium on Application of Ferroelectrics* (Nara, Japan). Edited by G. White and T. Tsunumi. Institute of Electrical and Electronics Engineers, New York, 2002.
[10]J. E. Smay, J. Cesarano, B. A. Tuttle, and J. A. Lewis, "Piezoelectric Properties of 3−*X* Periodic $Pb(Zr_xTi_{1-x})O_3$–Polymer Composites," *J. Appl. Phys.*, **92** [10] 6119–27 (2002).
[11]S. C. Danforth and A. Safari, "Solid Freeform Fabrication: Novel Manufacturing Opportunities for Electronic Ceramics"; pp. 183–88 in *ISAF '96* (East Brunswick, NJ, 1996). Institute of Electrical and Electronics Engineers, New York, 1996.
[12]A. Bandyopadhyay, R. K. Panda, V. F. Janas, M. K. Agarwala, S. C. Danforth, and A. Safari, "Processing of Piezocomposites by Fused Deposition Technique," *J. Am. Ceram. Soc.*, **80** [6] 1366–72 (1997).
[13]M. Allahverdi, S. C. Danforth, M. Jafari, and A. Safari, "Processing of Advanced Electroceramic Components by Fused Deposition Technique," *J. Eur. Ceram. Soc.*, **21**, 1485–90 (2001).
[14]J. Cesarano III and P. Calvert, "Freeforming Objects with Low-Binder Slurry," U.S. Pat. No. 6 027 326, 2000.
[15]J. Cesarano III, R. Segalman, and P. Calvert, "Robocasting Provides Moldless Fabrication from Slurry Deposition," *Ceram. Ind.*, **148** [4] 94–102 (1998).
[16]J. E. Smay, J. Cesarano III, and J. A. Lewis, "Colloidal Inks for Directed Assembly of 3-D Periodic Structures," *Langmuir*, **18** [14] 5429–37 (2002).
[17]J. E. Smay, J. Cesarano III, and J. A. Lewis, "Colloidal Inks for Directed Assembly of 3-D Periodic Structures," *Langmuir*, **18** [14] 5429–37 (2002).
[18]J. S. Reed, *Principles of Ceramics Processing*, 2nd ed. Wiley, New York, 1995.
[19]R. E. Newnham, D. P. Skinner, and L. E. Cross, "Connectivity and Piezoelectric–Pyroelectric Composites," *Mater. Res. Bull.*, **13**, 525–36 (1978). □